**Short Contribution**

# Co-tidal and Co-range Charts for the East China Sea and the Yellow Sea Derived from Satellite Altimetric Data

Tetsuo Yanagi, Akihiko Morimoto and Kaoru Ichikawa

*Department of Civil and Ocean Engineering, Ehime University, Matsuyama 790, Japan*

**Co-tidal and co-range charts of eight major constituent tides in the East China Sea and the Yellow Sea are drawn from the results of the harmonic analysis of TOPEX/POSEIDON altimetric data. Those of $M_2$, $S_2$, $K_1$ and $O_1$ constituents agree well with the traditional ones estimated from tide gauge data at coastal stations. Those of $N_2$ and $K_2$ are similar to those of $M_2$ constituent and those of $P_1$ are similar to $K_1$ constituent, respectively. The amplitude of $S_a$ constituent is large and its phase leads in the shallow part of the East China Sea and the Yellow Sea. The altimetric data from TOPEX/POSEIDON manifest very useful not only in the open ocean dynamics study but also in the coastal ocean dynamics study including tidal phenomena.**

## 1. Introduction

Satellite altimetric data have been very useful for the study of open ocean dynamics (e.g. Ichikawa and Imawaki, 1994). For the analysis of long-term variability in the ocean, the tidal models devised by Schwiderski (1980), based on numerical calculation, or by Cartwright and Ray (1990), on the basis of Geosat altimetric data, have been used in order to eliminate the tidal signal from the altimetric data. Recently, Ma *et al*. (1994) developed the method by Cartwright and Ray (1990) and obtained the tidal harmonic constants at $3° \times 3°$ over the world on the basis of TOPEX/POSEIDON altimetric data. Ma *et al*. (1994) assumed the same amplitude and phase in the horizontal scale of $3° \times 3°$ because they wanted to increase the temporal resolution by including several satellite tracks in one mesh of $3° \times 3°$. Their model is called the CSR model, and is now usually used to eliminate the tidal signal from the altimetric data in the open ocean dynamics study.

However, we cannot use their results directly in coastal seas, such as the East China Sea and the Yellow Sea (Fig. 1(a)), where the tidal waves show very complicated small scale features such as some amphidromic points and a very large horizontal gradient of tidal amplitude within the scale $3° \times 3°$ (Nishida, 1980).

In this paper, we propose a procedure by which we can estimate the tidal signal correctly from the altimetric data in the coastal sea; i.e. we carry out the tidal harmonic analysis using the altimetric data. As an example, we will take the East China Sea and the Yellow Sea where the tidal signal reaches several meters, and will estimate the tidal harmonic

constants of eight major constituents there; $M_2$, $S_2$, $N_2$, $K_2$, $K_1$, $O_1$, $P_1$ and $S_a$.

## 2. Altimetric Data

The satellite TOPEX/POSEIDON was launched in August 1992. It has continued to acquire the altimetric data approximately every 10 days along 7 observation lines in the East China Sea and the Yellow Sea, as shown in Fig. 1(b). The data are provided as the Merged Geophysical Data Record (MGDR) by the Physical Oceanography Distributed Active Archive Center at Jet Propulsion Laboratory, U.S.A. In the present analysis, we only used the data obtained TOPEX altimeter from Cycle 1 (September 1992) to Cycle 108 (August 1995) because there was an unknown bias in the order of 20 cm between the TOPEX and POSEIDON altimeters. (This problem was solved by NASA in July 1996, and so we can now also use POSEIDON data.)

Standard data corrections including electromagnetic bias correction, ionospheric correction, dry and wet trospheric correction and solid earth tide correction were made using the values provided in the MGDR. We did not, however, carry out any procedure to remove the radial orbit error, because such correction may cause omission of the tidal component. The radial orbit error has a wave length of the circumference of the earth. Its value is about 3 cm (Fu *et al*., 1994), which is very small compared to the tidal signal in the East China Sea and the Yellow Sea. Another important signal related to the sea surface dynamic topography may also be missed by this correction.

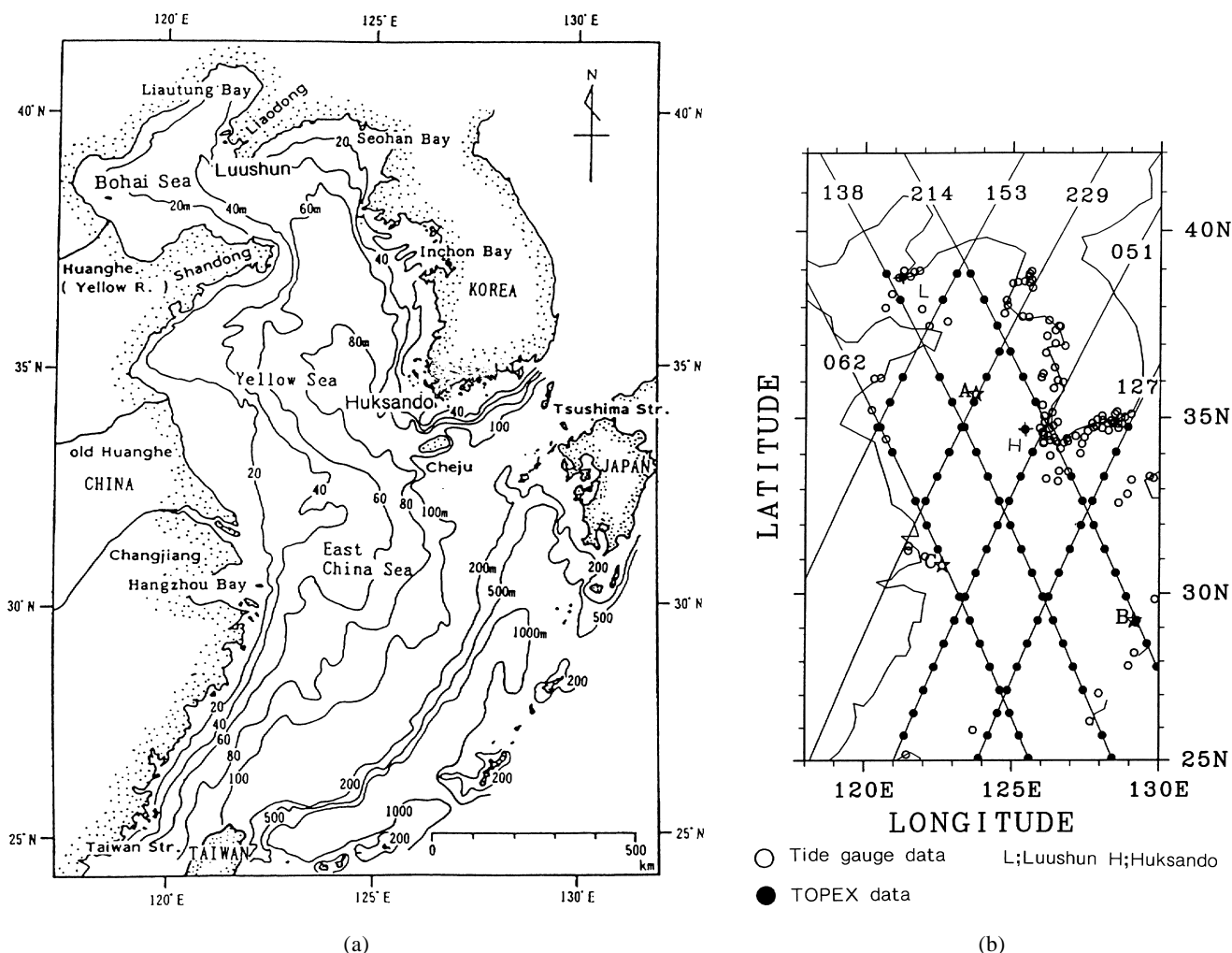The data of both ascending and descending tracks are

Fig. 1. The East China Sea and the Yellow Sea (a) and the observation lines of TOPEX/POSEIDON (b). A, B and C denotes the points where the results by TOPEX altimetry are compared with the tide gauge data, L denotes Luushun and H Huksando.

used after editing to remove the abnormal values due to instrument malfunction. Next, we remove the extreme altimetric values larger than ±5 m from the temporal mean of all data, because even the maximum spring tide can reach about 4 m in the East China Sea and the Yellow Sea. Initially, data are obtained about every second at intervals of about 6.2 km along the satellite tracks, but the data points differ every cycle. Hence, we linearly interpolated observed data at the fixed points with 6.2 km intervals along the subsatellite track. This is the projection of the satellite track on the sea surface, as shown in Fig. 1(b).

The altimetric data after the initial correction $S(r, t)$ are expressed as follows:

$$S(r, t) = \tau(r) + \tau'(r, t). \qquad (1)$$

Here $\tau(r)$ denotes the temporal mean of all data at station $r$,

$\tau'(r, t)$ the temporal deviation which includes the temporal variation of sea surface dynamic topography, tides, the temporal variation of radial orbit error and measurement error. We use $\tau'(r, t)$ for the harmonic analysis.

## 3. Harmonic Analysis

The tidal amplitudes at two representative stations along the coast in the Yellow Sea and the East China Sea; Luushun and Huksando (see Fig. 1(a)), are presented in Table 1. The $M_2$ constituent is the most dominant, and it is about 84 cm at Luushun and about 106 cm at Huksando. In the present analysis, we consider the tidal constituents whose amplitudes are larger than about 7 cm, that is, $S_a$, $K_1$, $O_1$, $P_1$, $M_2$, $S_2$, $N_2$ and $K_2$, because the level of accuracy of the TOPEX/POSEIDON altimeter is about 5 cm (Fu *et al.*, 1994). At first we did not include the $S_a$ constituent in this harmonic analysis, but this meant we could not obtain

accurate harmonic constants, because its amplitude in this area is large as shown in Table 1. We then decided to include the $S_a$ constituent although it is not an astronomical tidal constituent but a meteorological one.

The tidal harmonic analysis in this study was carried out using the aliasing period from each tidal constituent, because the sampling time of about 10 days by TOPEX is much longer than the tidal period of each constituent with the exception of $S_a$. The aliasing period $T_a$ from each tidal frequency $f$ is calculated by the following formula,

$$T_a = 1/(2nf_c \pm f), \qquad (2)$$

$$f_c = 1/2\Delta t$$

where $n$ denotes a integer part of $\Delta t \times f$ ($n = 19$ for $M_2$ tidal constituent), $f_c$ the Nyquist frequency and $\Delta t$ the sampling interval of 9.9156 days. The shortest aliasing period for each semi-diurnal and diurnal constituent is shown in Table 2. We must be aware that the accuracy of the period is critical for this harmonic analysis, because $T_a$ changes considerably according to a small change in $\Delta t$. This means that we have to use the double precision scheme in the computation. The necessary sampling time $T_d$ for separating two tidal con-

Table 1. Tidal amplitude at Luushun and Huksando (Ogura, 1933).

|  | Tidal amplitude (cm) | |
|---|---|---|
|  | Luushun | Huksando |
| $M_2$ | 83.5 | 106.2 |
| $S_2$ | 26.5 | 36.0 |
| $K_1$ | 22.4 | 24.2 |
| $O_1$ | 16.6 | 18.9 |
| $N_2$ | 16.1 | 21.1 |
| $K_2$ | 7.5 | 10.1 |
| $P_1$ | 6.4 | 7.7 |
| $S_a$ | 27.4 | 15.5 |

Table 2. Tidal periods and aliasing periods of major tidal constituents.

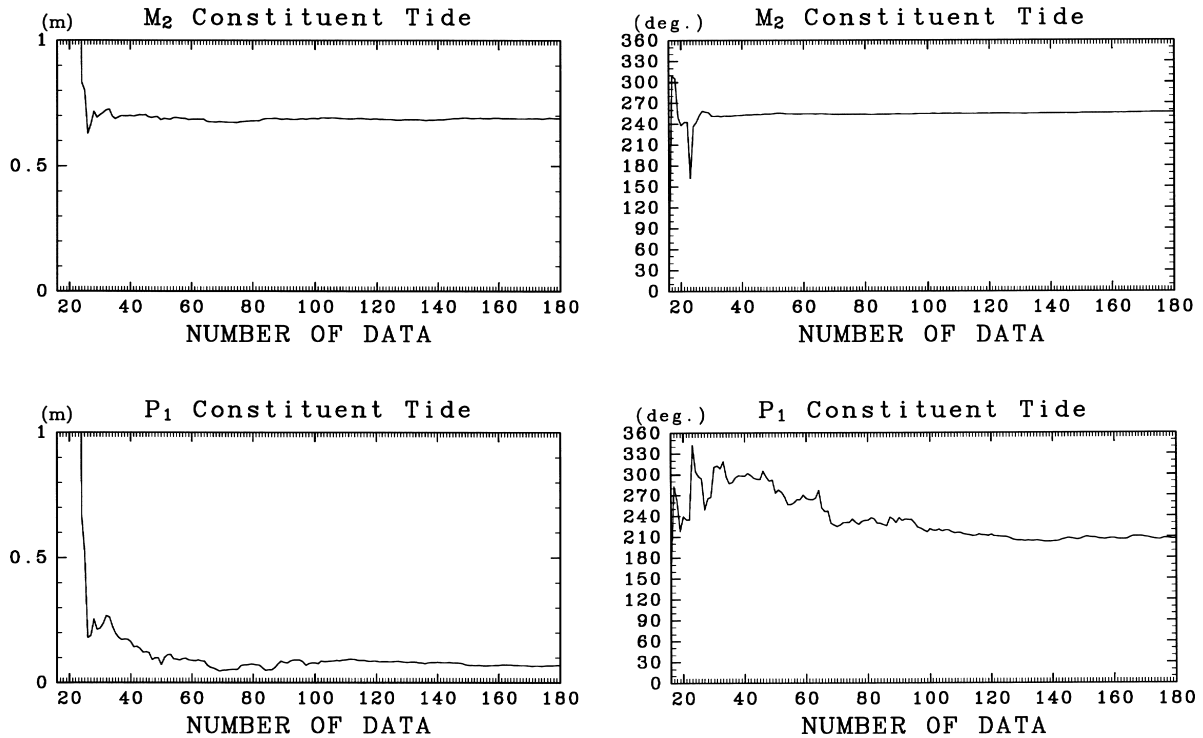| Tides | Period (hours) | Aliasing period (days) |
|---|---|---|
| $M_2$ | 12.420601 | 62.10 |
| $S_2$ | 12. | 58.74 |
| $N_2$ | 12.658384 | 49.52 |
| $K_2$ | 11.967235 | 86.61 |
| $K_1$ | 23.93447 | 173.22 |
| $O_1$ | 25.819342 | 45.71 |
| $P_1$ | 24.06589 | 88.89 |
| $S_a$ | 8765.821 (365.245 days) | |



Fig. 2. The dependence of obtained harmonic constants on the used data number.

Table 3. Comparison of observed harmonic constants at the coastal stations (observed), our model (estimated) and that of Ma *et al.* (1994) (CSR Model). The reference for phase lag is the longitude of the observation point. Stns. A, B and C are shown in Fig. 1(b).

| | | Stn. A | | Stn. B | | Stn. C | |
|---|---|---|---|---|---|---|---|
| | | Amplitude (cm) | Phase (deg.) | Amplitude (cm) | Phase (deg.) | Amplitude (cm) | Phase (deg.) |
| $M_2$ | | | | | | | |
| | Observed value | 83.0 | 63.0 | 56.0 | 207.0 | 120.0 | 299.0 |
| | Estimated value | 80.12 | 61.45 | 56.73 | 201.00 | 112.20 | 301.40 |
| | CSR model | 71.63 | 66.02 | 58.89 | 190.24 | 73.93 | 334.66 |
| $S_2$ | Observed value | 29.0 | 103.0 | 23.0 | 228.0 | 53.0 | 336.0 |
| | Estimated value | 28.72 | 99.60 | 25.20 | 217.61 | 55.86 | 355.86 |
| | CSR model | 28.88 | 103.77 | 23.96 | 222.78 | 34.77 | 2.65 |
| $K_1$ | Observed value | 14.0 | 302.0 | 22.0 | 211.0 | 27.0 | 196.0 |
| | Estimated value | 18.28 | 296.85 | 18.61 | 206.95 | 33.17 | 181.51 |
| | CSR model | 12.12 | 297.03 | 20.69 | 200.87 | 15.99 | 228.59 |
| $O_1$ | Observed value | 10.0 | 262.0 | 15.0 | 190.0 | 17.0 | 162.0 |
| | Estimated value | 15.34 | 270.03 | 13.81 | 182.41 | 15.17 | 167.07 |
| | CSR model | 9.76 | 262.29 | 16.52 | 171.28 | 11.67 | 183.38 |

stituents whose aliasing periods $T_1$ and $T_2$ are close to each other is calculated by the following formula:

$$T_d = T_1 \times T_2/(T_1 - T_2)/4 \qquad (3)$$

where $T_1$ is longer than $T_2$ and the number 4 means that at least 1/4 of the period is necessary to separate two constituents. From this formula, we understand that 0.7 year (271.7 days) is necessary to separate $M_2$ and $S_2$ constituents in the altimetric data, and 2.3 years (844.2 days) to separate $K_2$ and $P_1$ constituents.

The tidal harmonic analysis by the least squares method was directly carried out with unknown amplitudes and phases of eight tidal constituents. The obtained amplitudes and phases are the harmonic constants we want to know.

We checked the number of raw data necessary to obtain the stable harmonic constants using altimetric data at the crossover point of observation lines, where the number of obtained data is double. About 30 data (about 300 days) are necessary to obtain the stable harmonic constants of $M_2$, $S_2$, $O_1$, $K_1$ and $N_2$ constituents, and about 100 data (about 1000 days) for $K_2$ and $P_1$ constituents from Fig. 2 ($S_2$, $O_1$, $K_1$, $N_2$ and $K_2$ are not shown). These results verify Eq. (3).

We compare our results at three points, A, B and C (see Fig. 1(b)), with those obtained by the tide gauge data (A and C from Ogura, 1933; B from Maritime Safety Agency, 1983) and the results from Ma *et al.* (1994) at the same points. The results are shown in Table 3. Our results coincide well with those obtained by tide gauge data but the results by Ma *et al.* (1994) differ, e.g. the amplitude and phase at Stn. C. The reason for this difference is that Ma *et al.* (1994) av-

eraged the satellite data on a $3° \times 3°$ spatial scale, whereas we used the raw data from the subsatellite tracks directly.

## 4. Results

We have drawn the co-tidal and co-range charts of eight tidal constituents in the East China Sea and the Yellow Sea. First of all, tidal variation of the sea surface in the entire area by each tidal constituent is reconstructed using estimated tidal harmonics along the coast at the tide gauge stations, and those along the subsatellite tracks shown in Fig. 1(b). The tidal variations of the sea surface in the entire area are interpolated using the exponential function as follows,

$$\zeta(x) = \frac{\sum_i W(x, r_i) \zeta'(r_i)}{\sum_i W(x, r_i)}, \qquad (4)$$

$$W(x, r_i) = \exp\left\{\frac{(r_i - x)^2}{L^2}\right\}$$

where $\zeta(x)$ denotes the interpolated sea surface height, $x$ the position of interpolation, $r_i$ the position where tidal harmonics are already obtained, $\zeta'(r_i)$ the sea surface height at $r_i$ and $L$ (=100 km) the decorrelation radius, which is decided by the distance of neighboring subsatellite tracks. Therefore, the effect of coastal data at tide gauge stations is restricted to a very narrow strip (100 km) along the coast.

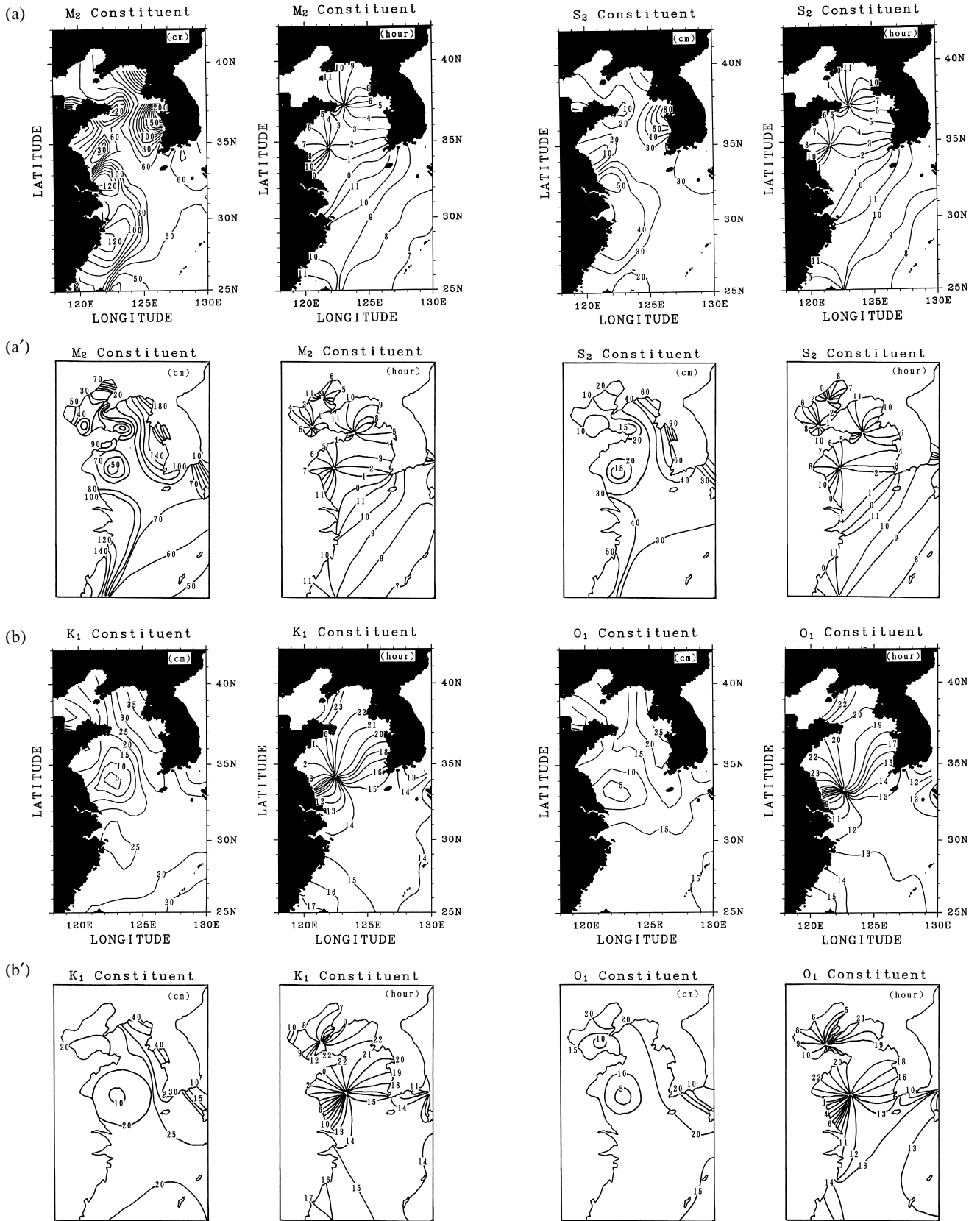The interpolation is carried out at every $5' \times 5'$ mesh

Fig. 3. The obtained co-tidal and co-range charts of M₂ and S₂ constituents (a), those of K₁ and O₁ constituents (b) and traditional charts ((a') and (b')) by Nishida (1980). The reference for phase lag is 135°E.
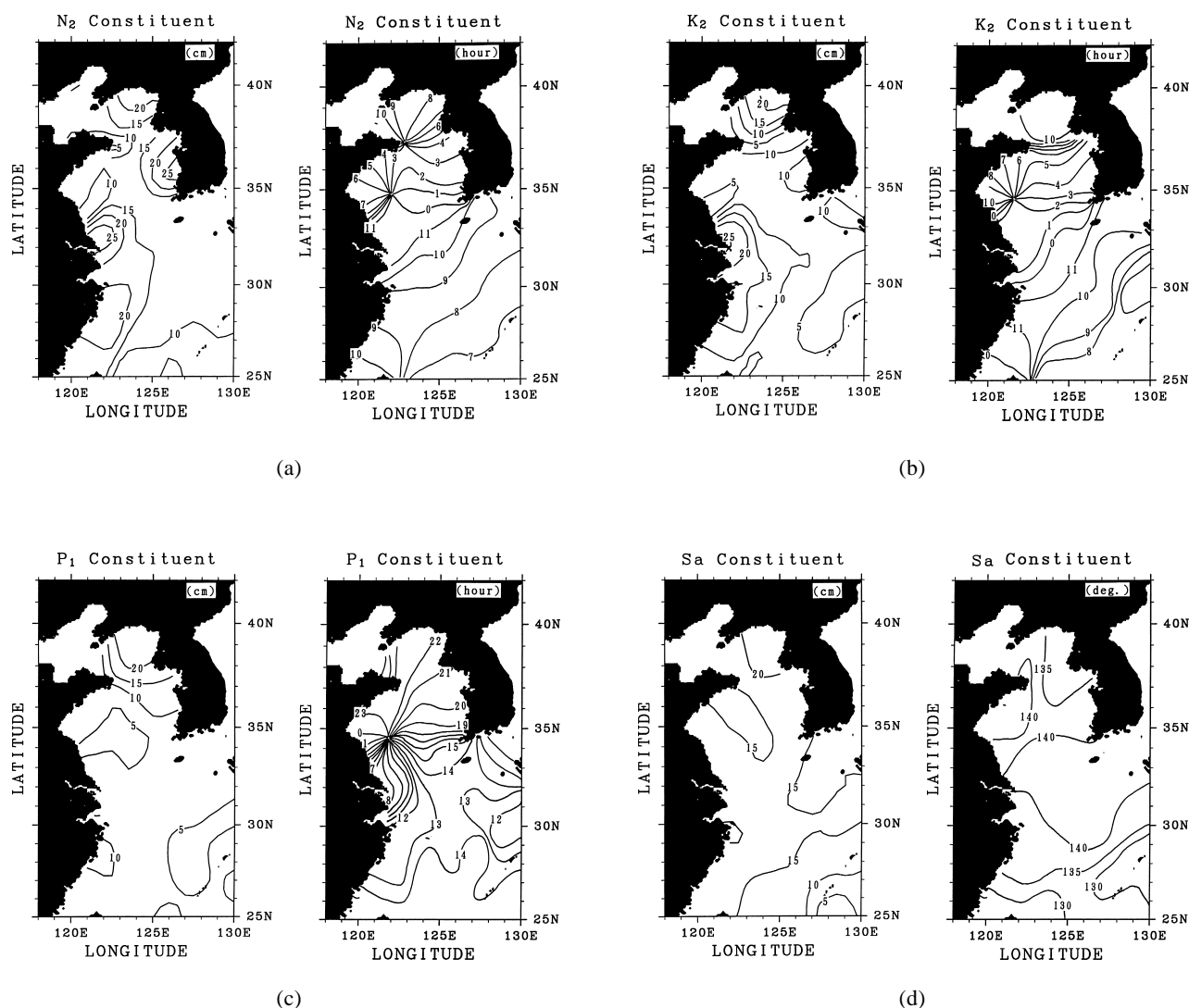
Fig. 4. The obtained co-tidal and co-range charts of $N_2$, $K_2$, $P_1$ and $S_a$ constituents. The phase of $S_a$ is degree and it is referred to the Vernal Equinox Day (around 21 March).

point. If there are not two observation stations within the circle of $1.5 \times L$, the interpolation is not carried out at that point. After the estimation of temporal variation of sea surface height in one tidal cycle, we carry out the tidal harmonic analysis at every $5' \times 5'$ mesh point in the entire area and obtain tidal harmonics there.

The obtained co-tidal and co-range charts of major four constituents, $M_2$, $S_2$, $K_1$ and $O_1$ are shown in Fig. 3 together with those estimated from tidal harmonics based only on coastal stations by Nishida (1980). The correlation between the figures is good with only small discrepancies. The co-tidal and co-range charts of four other constituents, $N_2$, $K_2$, $P_1$ and $S_a$ are shown in Fig. 4 without those by field observations because there are no published charts for these four constituents. The charts of $N_2$ and $K_2$ constituents resemble

to those of $M_2$ and $S_2$, and those of $P_1$ are similar to $O_1$ and $K_1$. Figure 4(d) is the first co-tidal and co-range chart of the $S_a$ constituent.

## 5. Discussions

The amplitude of the $S_a$ constituent is large and its phase early in the shallow area; they are small and late in the deep area, respectively, as shown in Fig. 4(d). The phase of $140°$ of the $S_a$ constituent means mid August, because it refers to the Vernal Equinox Day (around 21 March). These facts suggest that the main cause of the $S_a$ constituent in the East China Sea and the Yellow Sea is the sea water expansion and contraction due to seasonal variation of the sea surface heat flux. However, the largest amplitude of the $S_a$ constituent appears in Seohan Bay, on the northwestern coast of Korea,

which is not the shallowest part of this area. This fact suggests that the monsoon wind also affects the $S_a$ constituent there, that is, the strong southward wind during winter sets down the sea level at Seohan Bay and the northward wind during the summer sets up the sea level there (Yanagi and Takahashi, 1993).

We have compared our estimated co-tidal and co-range charts with those drawn by Ma *et al.* (1994). The root mean square difference of the two results for the $M_2$ constituent is more than 50 cm near the mouth of Changjiang and along the western coast of the Korean peninsula where the tidal signal is very large. This can also be inferred from Table 3, where the discrepancy between the results of tide gauge data and those by Ma *et al.* (1994) is very large at Stn. C near the mouth of Changjiang.

We have also compared our results with those of Mazzega and Bergé (1994) who produced the tidal map on a $0.5° \times 0.5°$ mesh in Asian semienclosed seas, by inverting combined sets of tide gauge harmonic constants and a reduced set of TOPEX/POSEIDON altimetric data. The two results on $M_2$ constituent coincide well in the East China Sea and the Yellow Sea. However, there is no amphidromic point for the $K_1$ constituent in the Yellow Sea on Mazzega and Bergé's chart (1994), though there is an amphidromic point in both our result and that of Nishida (1980). Our result is better than that of Mazzega and Bergé (1994) on this point. The reason of this discrepancy is not clear but may be due to the short analysis period of 210 days used by Mezzaga and Bergé (1994). Anyway, the results of our study and those of Mazzega and Bergé (1994) show that the altimetric data are very useful, not only in the open ocean dynamics study, but also in the coastal ocean dynamics study including tidal phenomena.

Recently, it has been recommended that the result of Le Provost *et al.*'s (1994) numerical model be used to eliminate the tidal signal from the altimetric data in the coastal sea. We will carry out a detailed comparison of our data with those of Le Provest *et al.* (1994) and Mazzega and Bergé (1994) in the near future.

## References

Cartwright, D. E. and R. D. Ray (1990): Oceanic tides from Geosat altimetry. *J. Geophys. Res.*, **95**(C3), 3069–3090.

Fu, L. L., E. J. Christensen, C. A. Yamarone, Jr., M. Lefebvre, Y. Menard, M. Dorrer and P. Escudier (1994): TOPEX/POSEIDON mission overview. *J. Geophys. Res.*, **99**(C12), 24,369–24,381.

Ichikawa, K. and S. Imawaki (1994): Life history of a cyclonic ring detached from the Kuroshio Extension as seen by the Geosat altimeter. *J. Geophys. Res.*, **99**(C12), 15,953–15,966.

Le Provost, C., M. L. Genco and F. Lyard (1994): Spectroscopy of the world ocean tides from a finite element hydrodynamic model. *J. Geophys. Res.*, **99**(C12), 24,777–24,797.

Ma, X. C., C. K. Shum, R. J. Eanes and B. D. Tapley (1994): Determination of ocean tides from the first year of TOPEX/POSEIDON altimeter measurements. *J. Geophys. Res.*, **99**(C12), 24,809–24,820.

Maritime Safety Agency (1983): Table of Tidal Harmonic Constants. 172 pp.

Mazzega, P. and M. Bergé (1994): Ocean tides in the Asian semienclosed seas from TOPEX/POSEIDON. *J. Geophys. Res.*, **99**(C12), 24,867–24,881.

Nishida, H. (1980): Improved tidal charts for the western part of the North Pacific Ocean. *Report of Hydraulic Researches*, **15**, 55–70.

Ogura, S. (1933): The tides in the seas adjacent to Japan. *The Bulletin of the Hydrographic Department*, **7**, 1–189.

Schwiderski, E. W. (1980): On charting global ocean tides. *Rev. Geophys.*, **18**(1), 243–268.

Yanagi, T. and S. Takahashi (1993): Seasonal variation of circulations in the East China Sea and the Yellow Sea. *J. Oceanogr.*, **49**, 503–520.